Structure, Vol. 13, 225–234, February, 2005, ©2005 Elsevier Ltd All rights reserved. DOI 10.1016/j.str.2004.12.009

Design of a Heterospecific, Tetrameric, 21-Residue Miniprotein with Mixed α/β Structure

Mayssam H. Ali,[1,4] Christina M. Taylor,[2,4] Gevorg Grigoryan,[2] Karen N. Allen,[3] Barbara Imperiali,[1,2] and Amy E. Keating[2,*]

[1]Department of Chemistry
Massachusetts Institute of Technology
77 Massachusetts Avenue
Cambridge, Massachusetts 02139

[2]Department of Biology
Massachusetts Institute of Technology
77 Massachusetts Avenue
Cambridge, Massachusetts 02139

[3]Department of Physiology and Biophysics
Boston University School of Medicine
715 Albany Street
Boston, Massachusetts 02118

Summary

The study of short, autonomously folding peptides, or "miniproteins," is important for advancing our understanding of protein stability and folding specificity. Although many examples of synthetic α-helical structures are known, relatively few mixed α/β structures have been successfully designed. Only one mixed-secondary structure oligomer, an α/β homotetramer, has been reported thus far. In this report, we use structural analysis and computational design to convert this homotetramer into the smallest known α/β-heterotetramer. Computational screening of many possible sequence/structure combinations led efficiently to the design of short, 21-residue peptides that fold cooperatively and autonomously into a specific complex in solution. A 1.95 Å crystal structure reveals how steric complementarity and charge patterning encode heterospecificity. The first- and second-generation heterotetrameric miniproteins described here will be useful as simple models for the analysis of protein-protein interaction specificity and as structural platforms for the further elaboration of folding and function.

Introduction

Miniproteins are short polypeptides, typically having fewer than 40 residues, that adopt specific, discrete folds in aqueous solution (Imperiali and Ottesen, 1999). Many miniproteins have been described in the literature, including α-helical coiled coils and helical bundles (Hill et al., 2000), mixed α/β motifs (Dahiyat and Mayo, 1997; Mezo et al., 2001b ; Struthers et al., 1996), predominantly-β motifs (Cochran et al., 2001; Kortemme et al., 1998; Ottesen and Imperiali, 2001), and other folds (Neidigh et al., 2002; Zondlo and Schepartz, 1999). Some of these miniproteins are derived by reducing naturally occurring protein folds to a minimal folding core, whereas others have been designed de novo, either by visual inspection or with the use of computational methods. Miniproteins have served as scaffolds for ligand and metal binding, as well as for the introduction of catalytic activity (Ghirlanda et al., 1998; Lombardi et al., 2000; Moffet et al., 2000). Miniproteins, and coiled-coil miniproteins in particular, have been successfully utilized in materials science for the introduction of nanoscale structure and organization, often with "switchable" physical properties (Petka et al., 1998; Ryadnov and Woolfson, 2003). Heterooligomeric peptides are particularly useful in these contexts, as they provide a mechanism for integrating units with distinct properties. We are interested in designing heterooligomeric miniproteins both for potential applications and for fundamental investigations of how protein-protein interaction specificity is encoded in sequence and structure.

The small size of miniproteins provides several advantages for studying protein folding and association. First, the sequence-structure relationship is simplified. There are fewer variables available in miniproteins to encode properties of interest, and as a consequence these variables can be more systematically dissected. Second, miniproteins can be synthesized chemically, providing a straightforward method to test sequence variants including both natural and nonnatural amino acids. Chemical synthesis also enables the facile introduction of biophysical probes such as fluorophores. Finally, the small size of miniproteins renders them amenable to computational analyses, including structure design and the simulation of protein folding (Dahiyat and Mayo, 1997; Harbury et al., 1998; Snow et al., 2002; Zagrovic and Pande, 2003).

Numerous short homooligomeric miniproteins have been described, the majority of which are coiled coils and helical bundles. There are fewer examples of heterospecific systems, although a number of heterodimeric (Keating et al., 2001; McClain et al., 2001; Moll et al., 2001; O'Shea et al., 1993; Zhou et al., 1994), heterotrimeric (Lombardi et al., 1996; Nautiyal et al., 1995; Schnarr and Kennan, 2003), and heterotetrameric (Fairman et al., 1996; Sia and Kim, 2001) coiled-coil peptides have proven useful for protein engineering applications (Hodges, 1996; Ryadnov and Woolfson, 2003). Coiled coils consist of a variable number of α helices associated in a bundle with a slight superhelical twist. An "acid/base" strategy, in which heterospecificity is obtained by patterning the residues at the hydrophobic/hydrophilic interface of paired helices with complementary charged residues, has been shown to have great utility for encoding specific structure in coiled coils (Fairman et al., 1996; O'Shea et al., 1993). Steric complementarity between juxtaposed residues in the hydrophobic core has also been used to impart heterospecificity (Kashiwada et al., 2000; Monera et al., 1996).

Studies of designed heterooligomeric coiled-coil miniproteins have enriched our understanding of how specificity is achieved in naturally occurring proteins such as the transcription factors Fos and Jun (O'Shea et al., 1992). The shortest heterooligomeric miniprotein previously reported in the literature consists of 21 amino acids and forms a tetrameric coiled coil in solution (Fairman et al., 1996). It was used to test the influ-

*Correspondence: keating@mit.edu

[4]These authors contributed equally to this work.

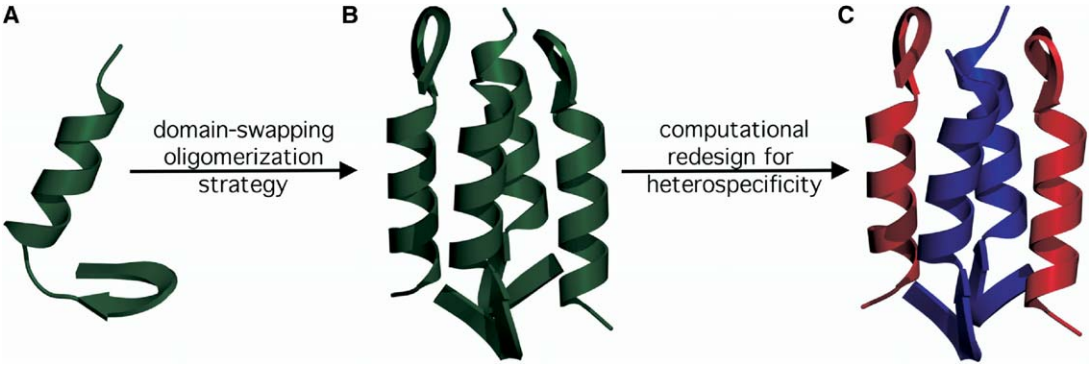

Figure 1. The Design History of the BBA Heterotetramers

(A) NMR structure of BBA5, an autonomously folding 23-mer designed to adopt the α/β fold of a zinc finger (Struthers et al., 1996, 1998).
(B) X-ray crystal structure of BBAT2, a homotetrameric derivative of BBA5 (Ali et al., 2004).
(C) X-ray crystal structure of BBAhetT1, a heterotetrameric miniprotein derived from BBAT2 by computer-aided design based on the structure of BBAT2 (this study).

ence of side chain length on charge-charge interactions. At this time, the structure of this complex has not been reported. In fact, relatively few designed heterospecific miniproteins have been characterized by NMR or X-ray crystallography, resulting in an incomplete understanding of the structural basis of heterospecificity (Keating et al., 2001; Marti et al., 2000; Nautiyal and Alber, 1999).

The miniproteins BBAT1 and BBAT2 (Figure 1B) are 21-residue homotetramers in which each monomer adopts a mixed $\beta\beta\alpha$ (BBA) secondary structure (Mezo et al., 2001a, 2001b). BBAT1 and BBAT2 are derived from the monomeric α/β miniprotein BBA5 (Figure 1A), a de novo designed metal ion-independent zinc finger (Struthers et al., 1996, 1998). BBAT1 was selected from a small library of BBA5 derivatives by means of a fluorescence-based quenching assay. A shortened loop between α and β subunits in BBAT1 precludes intramolecular burial of the hydrophobic surfaces and results in self-association to a homotetramer. BBAT2 is a more stable derivative of BBAT1 having D-alanine in place of the "hinge" glycine at position 9. The X-ray crystal structure of BBAT2 was recently reported (Ali et al., 2004), revealing a novel architecture with certain structural elements reminiscent of a tetrameric coiled coil. As in coiled coils, the central core of the BBAT2 tetramer is formed by association of the hydrophobic face of each monomer, including significant contributions from the helical portion. The hydrophobic core consists of five palindromic layers, each layer composed of one side chain from each monomer, similar to the core layers found in coiled coils. Furthermore, both apolar and polar residues are located along the intermonomer interfaces. Unlike a typical four-stranded coiled coil, however, the superhelical twist of BBAT2 is right-handed, and the "knobs-into-holes" packing that characterizes coiled coils (Walshaw and Woolfson, 2001) is not observed. Despite these differences, we anticipated that strategies employed in the design of hetero-oligomeric coiled coils would be applicable to the design of a heterotetrameric BBA complex.

Herein we describe the computational design and characterization of two miniprotein complexes, BBAhetT1 and BBAhetT2. Our goal was to design pairs of short peptides that would adopt the overall backbone structure of the BBA homotetramer, but in a heterospecific A_2B_2-type complex with C_2 or pseudo-C_2 symmetry. We sought a stable and highly specific motif that could be used to probe sequence determinants of interaction specificity and that could serve as a scaffold for further elaboration of structure or function. The design strategy was motivated by the structure of BBAT2 and used computational methods to identify and rank mutations likely to impart both stability and heterospecificity. Solution characterization and a high-resolution X-ray structure confirmed the success of our design. The evolution of the BBA family from monomer to heterotetramer is summarized in Figure 1.

Results

Computational Design

Homotetramer BBAT2 is very sensitive to mutation. Many residues in this small motif have multiple roles in determining specificity and stability, and seemingly minor sequence changes can lead to loss of structure or aggregation (Ali, 2004; McDonnell, 2001; McDonnell and Imperiali, 2002). We therefore adopted a stepwise strategy whereby the effects of mutations to core and surface sites were modeled and evaluated independently. An empirical, molecular mechanics-based energy function was used to identify suitable sites for mutation and to evaluate sequence substitutions at the chosen sites. Each sequence was modeled as a heterotetramer (giving E_{ABAB}), as two homotetramers (giving E_{AAAA} and E_{BBBB}) and as an unfolded monomer (giving E_{unfold}). We sought sequences with large values for both stability ($E_{unfold} - E_{ABAB}$) and specificity ($E_{AAAA} + E_{BBBB} - 2E_{ABAB}$).

The hydrophobic core of BBAT2 consists of five palindromic layers. The three unique layers are layer A (composed of residues 3 and 20), layer B (composed of residues 8 and 16), and layer C (composed of residues 12 and 12′). To identify sites for mutation, layers B and C were analyzed in detail. Calculations were carried out to select residues at positions 12, 8, and 16 that would

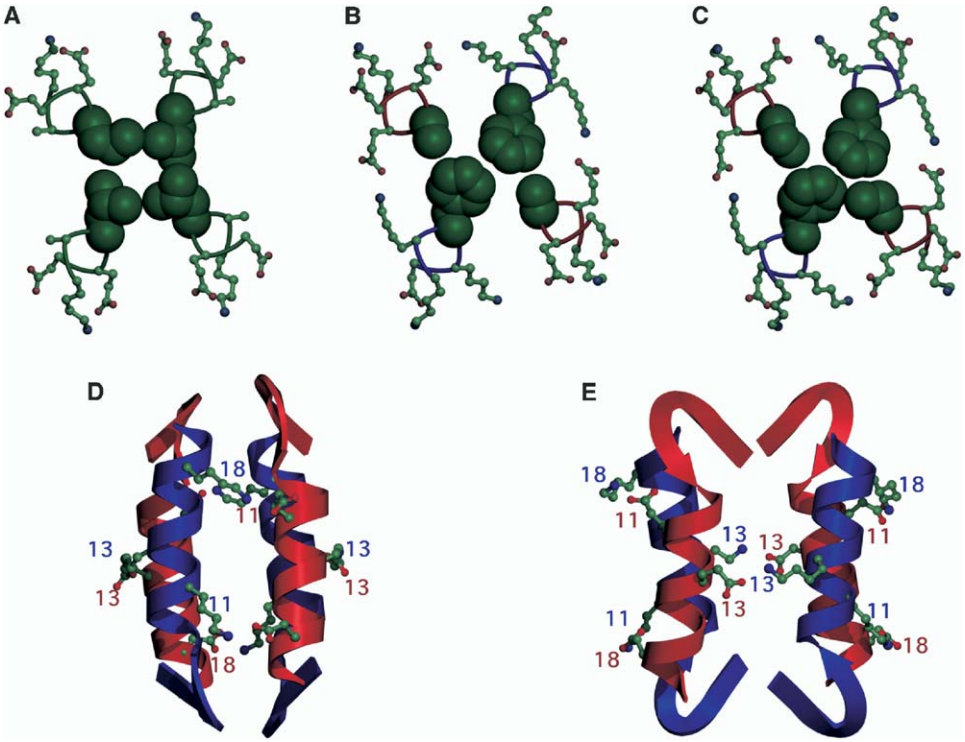

Figure 2. Design of Heterospecificity

(A–C) Core redesign.

(A) Four leucines at position 12 in BBAT2 pack poorly in the hydrophobic core (Ali et al., 2004).

(B) Ala was predicted to pack well against Phe in the core of a heterotetramer, and to disfavor homotetrameric states.

(C) The stability of the heterotetramer was improved and specificity was retained when Abu was substituted for Ala in BBAhetT2.

(D–E) Surface redesign. Positions 11, 18, and 13 of BBAT2 are Glu, Gln, and Ala, respectively. Calculations suggested that Asp or Lys at position 18 could form salt-bridging interactions with Glu or Lys at position 11, and that Lys or Glu residues at position 13 on adjacent subunits could also interact favorably, as shown. (D) and (E) are two views of the designed complex, rotated 90° around the tetramer axis with respect to one another.

impart heterospecificity. The largest predicted specificities came from substitutions at position 12. More qualitative analyses also indicated that position 12 was a good candidate for mutation. For example, a small fraction of leucines at this site in BBAT2 were modeled with alternate conformations in the three crystal structures, suggesting a nonoptimal fit of the side chains at this site in the homotetramer.

The most heterospecific sequences from the position 12 calculations systematically suggested a "large/small" design strategy, with two monomers contributing a bulky residue that could not be accommodated in the core of a homotetramer and two others contributing a small side chain that could not form good packing interactions in a homotetramer. Models of many different "large/small" combinations (e.g., Trp/Ala, Trp/Ser, Trp/Thr, Phe/Ala, Tyr/Val) indicated that these residues could be accommodated in a heterotetramer. Two different backbone structures for BBAT2 were used in the design calculations (see Experimental Procedures). On one backbone, Trp/Ala combinations were predicted to give the highest heterospecificity at positions 12 and 12′; on the other, Phe/Ala pairs were the most heterospecific. Phe/Ala pairs were computed to be more stable than Trp/Ala on both backbones. Furthermore, core side chains in the predicted L12F/L12A heterotetramer could be accommodated in statistically common rotamers (Dunbrack and Cohen, 1997; Dunbrack and Karplus, 1993). A peptide pair having Phe at position 12 in one chain and Ala at position 12 in the other chain was therefore selected for experimental analysis (Figure 2B).

Structural analysis, as well prior studies of BBAT2 (Ali et al., 2004), were used to select surface sites for mutation. At the hydrophobic/hydrophilic interface, positions 13 and 18 (alanine and glutamine, respectively, in BBAT2) were previously mutated to methionine selenoxide without structural perturbation, suggesting that the introduction of a charged residue would be tolerated. Position 13 is directly across from position 13 of an adjacent monomer, and distances in BBAT2 indicated that an interchain interaction would be possible at this site between residues with long side chains. Position 18 is opposite position 11 (glutamate) of an adjacent monomer in the homotetramer; these two sites were also selected for redesign.

Computational selection for heterospecificity at the surface sites suggested placing residues of opposite charge at structurally opposed positions, reminiscent of similar interactions found in heterospecific coiled

Table 1. Sequences of Designed Peptides

		Hairpin								Helix											
Peptide		1	2	3	4	5	6	7	8	9	10	11	12	13	14	15	16	17	18	19	20	21	
BBAT2	Ac	Y	R	I	p	S	Y	D	F	a	D	E	**L**	A	K	L	L	R	Q	A	Z	G	NH_2
A-Ala	Ac	Y	R	I	p	S	Y	D	F	a	D	E	**A**	E	K	L	L	R	D	A	Z	G	NH_2
B-Phe	Ac	Y	R	I	p	S	Y	D	F	a	D	K	**F**	K	K	L	L	R	K	A	Z	G	NH_2
A-Abu	Ac	Y	R	I	p	S	Y	D	F	a	D	E	**B**	**E**	K	L	L	R	**D**	A	Z	G	NH_2
A-Leu	Ac	Y	R	I	p	S	Y	D	F	a	D	E	**L**	E	K	L	L	R	D	A	Z	G	NH_2
B-Leu	Ac	Y	R	I	p	S	Y	D	F	a	D	**K**	**L**	K	K	L	L	R	K	A	Z	G	NH_2

BBAhetT1 = $(A\text{-}Ala)_2(B\text{-}Phe)_2$
BBAhetT2 = $(A\text{-}Abu)_2(B\text{-}Phe)_2$

a = D-Ala, p = D-Pro, Z= DapBz, B=Abu

coils. The highest specificity scores were obtained for combinations having Glu and/or Asp at positions 11, 13, and 18 of one monomer, and Arg and/or Lys at opposing sites of adjacent monomers. Computed specificity rankings, in conjunction with a visual examination of the structures generated by side chain repacking, led to the selection of Glu/Lys or Asp/Lys pairs at position 13/position 13 and position 11/position 18 sites (Figures 2D and 2E).

Solution and Structural Characterization

Peptides A-Ala and B-Phe were synthesized, incorporating the core and surface changes suggested by the computational analysis (Table 1). The two peptides individually exhibited very weak circular dichroism (CD) spectra between 200 and 300 nm at 50 μM, indicating they have little secondary structure. By contrast, an equimolar mixture of A-Ala and B-Phe revealed an increase in ellipticity and a qualitatively different spectrum indicative of interhelical association (Zhou et al., 1992), as observed for homotetramers BBAT1 and BBAT2. The change in secondary structure upon mixing (Figure 3A) strongly supports the formation of a heterooligomeric complex. Thermal melts of the A-Ala/B-Phe complex, termed BBAhetT1, showed a cooperative-unfolding transition (Figure 3B). Furthermore, heterooligomerization was supported by a fluorescence-quenching assay (Figure 4). The molecular weights of BBAhetT1 and of the individual components were determined by sedimentation equilibrium analytical ultracentrifugation (AUC) experiments (Table 2). Peptides A-Ala and B-Phe were found to be monomeric at low concentrations, but BBAhetT1 was best described as a single tetrameric species. A tracer sedimentation equilibrium experiment (Rivas and Minton, 2003) further confirmed the heterospecificity of the interaction (Supplemental Data, Supplemental Table S1 available with this article online).

The designed combination of a "large/small" core packing motif and charge complementarity was suc-

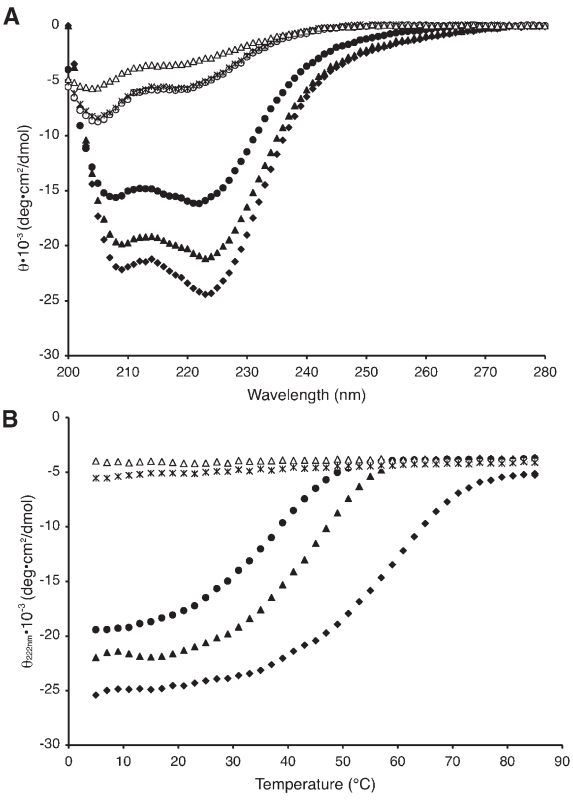

Figure 3. Solution Characterization of BBA Oligomers

(A) Circular dichroism spectra of A-Ala (○), A-Abu (*), B-Phe (Δ), BBAhetT1 (•), BBAhetT2 (▲), and BBAT2 (♦) with total peptide concentration of 50 μM.

(B) Thermal denaturation of A-Abu, B-Phe, BBAhetT1, BBAhetT2, and BBAT2 at 50 μM total peptide concentration; symbols as in (A).

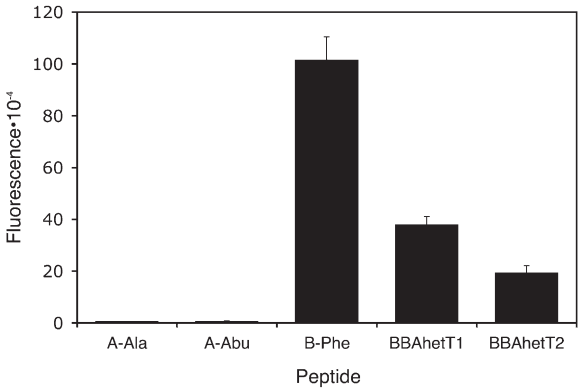

Figure 4. Fluorescence Quenching Experiments Demonstrating Heterospecific Interactions between A-Ala and B-Phe and A-Abu and B-Phe

Peptides were synthesized with a quencher (A-Ala and A-Abu) or fluorophore (B-Phe) label. Combinations of A-Ala and B-Phe (BBAhetT1) and A-Abu and B-Phe (BBAhetT2) exhibit fluorescence quenching. Error bars indicate standard deviations.

Table 2. AUC Results

Peptide	A-Ala	B-Phe	BBAhetT1	A-Abu	BBAhetT2
$\bar{\nu}^2$ (cm^3/g)[a]	0.7234	0.7510	0.7372	0.7248	0.7379
MW_{calc}	2561	2648	10418	2575	10446
NONLIN					
Best Model[b]	a	a	a	b	b
Sigma[c]	0.5012	0.5493	1.6758	0.4452	1.8010
MW_{obs}	2616	3208	9253	2336	9938
Stoichiometry[d]	1.0	1.2	3.6	0.9	3.8
SEDPHAT					
MW_{obs}	2703	3193	9393	2631	9491
Stoichiometry	1.1	1.2	3.6	1.0	3.6

[a] Partial specific volumes were calculated using the program SEDNTERP (Laue et al., 1992). Partial specific volumes of complexes were approximated as the average of the partial specific volumes of the individual components.
[b] Best model: a: Single species, B = 0. b: Single species, B $\neq$ 0.
[c] Sigma is related to the molecular weight by the equation $M = \frac{\sigma RT}{(1-\bar{\nu}\rho)\omega^2}$.
[d] Stoichiometry is defined as $(MW_{obs})/(MW_{calc})$. In the case of a mixture, MW_{calc} is the average of the calculated molecular weights of the components.

cessful in imparting heterospecificity to BBAhetT1. However, this complex is significantly destabilized relative to the parent homotetramer BBAT2. An analysis of computationally predicted structures indicated that a larger side chain could be accommodated in place of Ala in the "small" partner at position 12. Serine was predicted to result in more favorable van der Waals interactions relative to alanine at this site, but also in an overall reduction in stability. The nonnatural amino acid L-α-aminobutyric acid (Abu) was predicted to stabilize the tetramer by $\sim$4 kcal/mol, based on estimates of van der Waals and solvation contributions, and to retain high specificity for heterotetramerization. Peptide A-Abu, with an Ala to Abu substitution at position 12 (Table 1), was synthesized. The CD spectrum revealed that A-Abu has little secondary structure alone. An equimolar mixture of A-Abu and B-Phe gave a spectrum very similar to that observed for BBAhetT1, but with greater ellipticity at 208 and 222 nm. A complex of A-Abu and B-Phe, termed BBAhetT2, exhibited a cooperative thermal unfolding transition, and was considerably more stable to thermal denaturation than BBAhetT1 (Figure 3B). Heterooligomerization was confirmed by fluorescence quenching (Figure 4). AUC experiments indicated that equimolar mixtures of A-Abu and B-Phe are best described as a single tetrameric species (Table 2). By contrast, peptides A-Abu and B-Phe are both monomeric at 25 μM.

The 1.95 Å crystal structure of BBAhetT1 was solved by molecular replacement, using two monomers from BBAT2 as a search model (Table 3 and Figure 5). The overall fold (Figure 1C) is very similar to that of BBAT2, with an all-atom rms deviation of 1.76 Å and an all-backbone atom rms deviation of 0.71 Å. The similarity of the backbone structures indicates that the calculations were successful in identifying an alternative sequence compatible with the precise geometry of the homotetramer fold. The structure confirms that BBAhetT1 is a C_2-symmetric heterotetramer, as intended. The tetramer axis coincides with a perfect 2-fold screw axis in the crystallographic symmetry. The conformations of the designed side chains and their surrounding residues in the core are in excellent agreement with the calculated predictions (Figure 6). On the surface, two designed salt bridges between Glu 11 on A-Ala and Lys 18 on B-Phe are formed, with slightly different side chain conformations than predicted. Four other designed salt bridges are not present, but in each of these cases the designed residues participate in intertetramer crystal contacts that were not represented in the calculations (Figure 6).

Discussion

The design of miniproteins is challenging. Many residues in the BBA peptides play multiple structural roles, and single point mutations can affect the overall fold or solution properties. In our work, computational methods proved valuable for rapidly identifying mutations that would change the interaction specificity of BBAT2 while maintaining its overall structure. Calculations were used to identify possible sites for mutation as well as to find the best combination of residues for stabilizing a heterotetramer relative to competing homotetramers and the unfolded state. Despite the very large number of possible sequences, the first set of designed peptides that we tested exhibited the desired properties. The efficiency of this structure-based computational approach can be compared to the much slower process of performing an experimental selection or the iterative process of testing sequences suggested by visual inspection.

Computational protein design does have significant limitations. Modeling structural relaxation, particularly backbone flexibility, is challenging (Desjarlais and Handel, 1999; Harbury et al., 1993; Kuhlman et al., 2003). In the absence of a realistic model to describe relaxation, our method predicted that sequences with large groups in the core would be highly destabilized and not fold as homotetramers (Supplemental Tables S2 and S3). By contrast, our experiments revealed that B-Phe, an example of such a peptide, nevertheless associates to some extent in solution at high concentrations (data not shown). The strategy of designing holes in the core, rather than steric bulk, was significantly more effective at destabilizing the homotetramer state. Relaxation of side chain conformations in the calculations, and the use of multiple tetramer structures as templates in the

Table 3. X-Ray Statistics	
Data Collection Statistics[a]	
Unit cell (Å, °)	a = b = 41.70 c = 51.33 α = β = 90 γ = 120
Space group	$P3_121$
Wavelength (Å)	1.5418
Resolution (Å)	∞–1.95
Total/unique reflections	32,475/3,881
Completeness (%)	95.7 (100.0)
I/σ(I)	24.9 (7.1)
R_{merge}[b] (%)	5.8 (38.9)
Refinement Statistics	
Resolution (Å)	17.03–1.95
No. of reflections working/test set	3369/380
R_{work}[c]/R_{free}[d] (%)	22.2 / 24.0
Average B Factors (Å^2)	
Wilson plot	32.4
Amino acids	37.8
Water	55.5
RMS Deviations from Ideality	
Bond lengths (Å)	0.009
Angles (°)	1.5
Dihedral angles (°)	21.7

[a] Values for the outermost shell (2.02–1.95 Å) are shown in parentheses.
[b] $R_{merge} = \Sigma_{hkl}\Sigma_i|I_{hkl,i} - \langle I_{hkl}\rangle| / |\Sigma_{hkl}\Sigma_i|I_{hkl,i}|$, where $\langle I_{hkl}\rangle$ is the mean intensity of the multiple $I_{hkl,i}$ observations for symmetry related reflections.
[c] $R_{work} = \Sigma_{hkl}|F_{obs} - F_{calc}| / \Sigma_{hkl}|F_{obs}|$.
[d] $R_{free} = \Sigma_{hkl\ \Sigma T}|F_{obs} - F_{calc}| / \Sigma_{hkl}|F_{obs}|$, where the test set T includes 10% of the data.

design process, alleviated the problem of large steric clashes to some extent.

BBAhetT1 and BBAhetT2 are both less stable than BBAT2, indicating that specificity in this system comes from destabilization of the competing homotetramer states rather than stabilization of the heterotetramer. Charge patterning is an effective negative design strategy in some heterospecific coiled coils (O'Shea et al., 1993). However, we found that BBA peptides in which only the surface side chains are altered (A-Leu and B-Leu, Table 1) self-associate in solution (data not shown). Charge-charge repulsion in these systems is not sufficient to prevent the undesired states from forming under the conditions studied. A-Leu and B-Leu do, notably, preferentially form heterooligomers when mixed, as demonstrated by fluorescence quenching and CD experiments (data not shown). But a significant amount of additional heterospecificity in BBAhetT1 and BBAhetT2 is apparently derived from the core redesign and its role in disfavoring homotetramerization.

We observed excellent agreement of the backbone and core structure of BBAhetT1 with the computationally predicted design. The behavior of the designed charged residues in the crystal structure is more complex than predicted by the calculations. Notably, all but one of the computationally predicted surface residues were observed to have high temperature factors or multiple conformations in the BBAT2 or BBAhetT1 crystal structures, suggesting that the conformational preferences at these sites are not absolute. In addition, most of the designed side chains in the BBAhetT1 structure are involved in intertetramer interactions. At sites where BBAhetT1 surface residues do not participate in crystal contacts, the designed salt bridges form as predicted. Charged surface residues on BBAhetT1 are probably dynamic in solution and influenced by lat-

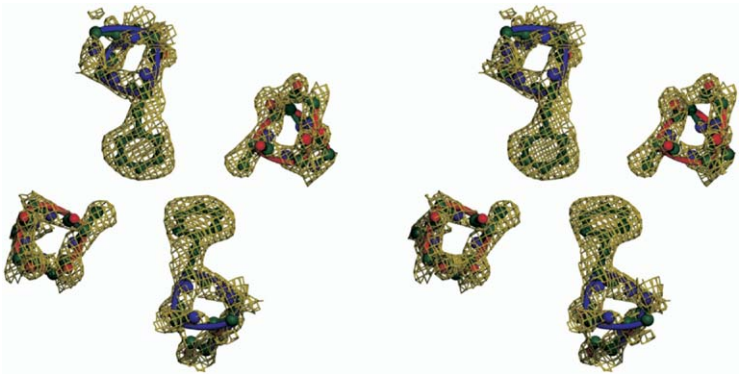

Figure 5. Stereo View of Layer C of BBAhetT1 with Composite-Omit Map Contoured at 1.0 σ

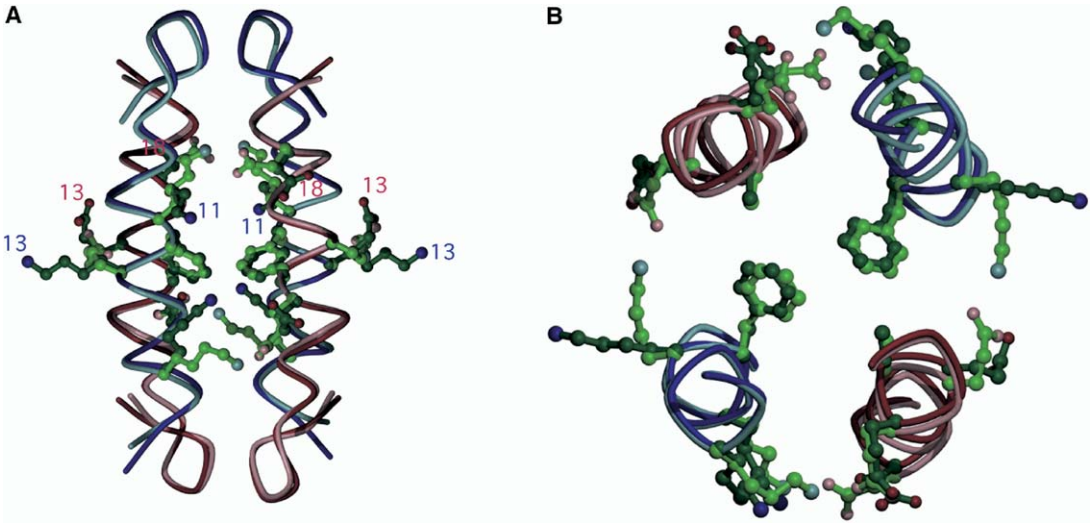

Figure 6. Crystal Structure of BBAhetT1 (Dark) Superimposed on the Predicted Designed Structure (Light)

Superimposed backbones are depicted as ribbons, with side chains at the designed positions 11, 12, 13, and 18 rendered as ball-and-stick models. Residues involved in intertetramer contacts are labeled.

(A) Entire backbone structure with designed side chains.

(B) The helical region of BBAhetT1 showing layer 12 and the designed surface residues.

tice contacts in the crystal. Information about whether the designed salt bridges form in solution would allow a more direct comparison with the calculations.

We used the native BBAhetT1 backbone to model the difference in energy between the predicted and the experimental structures of the heterotetramer. We approximated the experimental structure using native side chain chi angles but bond lengths and angles from CHARMM. The energy function used for design strongly favored the formation of salt bridges between acidic and basic surface residues, as observed in the sequence-selection calculations. Interestingly, when the side chain conformations were relaxed by minimization and the energies reevaluated using more accurate electrostatics functions (see Experimental Procedures), the difference between salt-bridge forming and nonsalt bridge forming configurations decreased dramatically. These calculations support a small energy gap between structures with different numbers of salt bridges, consistent with the high temperature factors and alternative conformations seen in the heterotetramer crystal structure.

Differences in the placement of residue Tyr 6, and other very minor differences between the design and the BBAhetT1 structure, resulted from simplifying assumptions of the computational method. For example, the incorrect prediction of Tyr 6 arose because the rotamer library used did not contain all of the experimentally observed side chain chi angles. In addition, even slight changes in backbone geometry (e.g., the 0.5 Å difference between the BBAT2 and the BBAhetT1 backbones) made significant differences in the correct placement of rotamers and in salt bridge formation. Predictive performance for Tyr 6 was improved when wild-type rotamers were included and the sequence was modeled using the correct heterotetramer backbone.

In conclusion, we have designed and characterized two compact, heterotetrameric, mixed α/β miniproteins, BBAhetT1 and BBAhetT2. Both were derived from a homotetrameric precursor using computational screening of many possible sequence/structure combinations. These tetramers constitute the first reported heterooligomeric α/β miniproteins, to our knowledge, and arguably are the most complex miniproteins designed thus far. The BBA family of peptides has proven to be quite remarkable. The power of small sequence changes to encode monomeric, homotetrameric, and heterotetrameric BBA variants, and to tune stability and specificity within each class, makes this system ideal for studying basic principles of protein structure. The study described here has established several ways that oligomerization specificity can be manipulated in the BBA peptides. Future work is likely to suggest others, and to lead to yet more novel architectures, activities and functions, all specified by a sequence of only 21 amino acids.

Experimental Procedures

Computational Design

All calculations, unless stated otherwise, used symmetry-generated tetramers from the crystal structures of two selenomethionine mutants of BBAT2 (1SNA and 1SNE). In the case of a residue having alternate conformations, the first listed conformation was used. Methionine selenoxide residues were modeled as alanines. Allowed side chain conformations were defined by the backbone-dependent rotamers of Dunbrack (Dunbrack and Cohen, 1997; Dunbrack and Karplus, 1993), using default bond lengths and angles from CHARMM param19 (Brooks et al., 1983). Nonstandard amino acids added were: D-alanine (D-Ala), D-proline (D-Pro), benzoylated L-α,β-diaminopropionic acid (DapBz), and L-α-aminobutyric acid (Abu). The angle CH1E-CH2E-NH1, with a force constant of 100.0 and equilibrium geometry of 109.5, and the improper dihedral NH1-H-C-CH2E, with a force constant of 750.0, multiplicity of 0, and mini-

mum geometry of 0.0, were added to the CHARMM 19 parameter set for DapBz (Ali et al., 2004). Rotamers of Abu were modeled using rotamers of serine (Dunbrack and Karplus, 1993).

Design energies were defined as the sum over all self energies plus the sum over all unique residue-residue energies for all flexible sites. The self energies include intra-side chain interactions, as well as interactions with the backbone and nondesigned side chains; the pair-wise energies include the interactions of a particular side chain with another side chain. The van der Waals radii from CHARMM param19 were scaled by 90% to accommodate discrete rotamer conformations. The total van der Waals energy was also scaled by 90%. Torsion energies were computed using param19. The pair-wise electrostatic energy was calculated using a coulombic function with ε = 4r for polar-polar interactions, 8r for polar-charged interactions, and 16r for charged-charged interactions; for self energies, ε = 4r was used. Both the self and pair-wise solvation energies were calculated using an Effective Energy Function (EEF1), (Lazaridis and Karplus, 1999) with reference/free energies as published except for NH3 (–10/–10), NC2 (–7.5/–7.5), OC (–5.33/–5.85). The unfolded state was modeled by treating each residue in turn as the central residue, X, in a Gly-Gly-X-Gly-Gly pentapeptide. The backbone structure employed was that of residue X and the two residues preceding and following X in the crystal structure. The side chain of residue X was modeled as an ensemble average of all possible rotamer states, employing the same energy function used for the folded states.

Sequences were either enumerated or sampled using a Monte Carlo search algorithm. The Monte Carlo search algorithm employed 64 cycles of 1500 steps with a linear temperature gradient from 300 to 200 K. For each sequence, the side chains were placed onto one or more backbones in an optimal configuration using a DEE/A* algorithm (Desmet et al., 1992; Goldstein, 1994). Two quantities were evaluated: the stability ($E_{unfold} - E_{ABAB}$) and the specificity ($E_{AAAA} + E_{BBBB} - 2E_{ABAB}$). Sequences were ranked according to these two scores, and those with high stability and specificity on both of the backbones used were considered for further analysis. For selected models, the energies were reevaluated with a function including the following terms: CHARMM param19 van der Waals energy (100% radii), Coulomb energy evaluated with a dielectric constant of 4, polarization energy for transfer from a protein/environment dielectric of 4/4 to 4/80, and a surface tension term computed as the solvent accessible surface area multiplied by 7 cal/mol•Å^2. The polarization energy was computed with a Generalized Born model (Dominy and Brooks, 1999) that used PEP to solve for Born radii (Beroza and Case, 1998). A version of the energy function in which the Generalized Born reaction field energies were substituted by EEF desolvation energies was also used. Models were evaluated both before and after 10 steps of steepest descent minimization (maintaining a fixed backbone) to relieve side chain steric clashes.

Peptide Synthesis

Peptides were prepared by standard Fmoc-based solid-phase peptide synthesis as in Ali et al. (2004). Identity was confirmed by electrospray mass spectroscopy (PerSeptive Biosystems) and purity by analytical HPLC (>95%).

Circular Dichroism

CD spectra from 300 to 200 nm were collected at 25°C in duplicate or triplicate on an Aviv circular dichroism spectrometer Model 202 using strain-free quartz cells having a path length of 0.1 cm and an averaging time of 5 s. Peptides were dissolved in degassed buffer (50 mM sodium phosphate, 100 mM NaCl, [pH 7.2]), and concentrations were determined using the method of Edelhoch (1967). Melting experiments involved monitoring $[\theta]_{222}$ using a 30 s averaging time, 90 s equilibration time, and temperature increments of 2°C from 5°C to 80°C.

Fluorescence Quenching

Peptides were synthesized with a 3-nitrotyrosine quencher at position 6 (A-Ala and A-Abu) or an anthranilamide fluorophore at position 20 (B-Phe). 12.5 μM samples were prepared of fluorophore- or quencher-labeled peptides in 10 mM phosphate buffer, [pH 7.2]. Combination samples comprised 12.5 μM fluorophore-labeled peptide plus 12.5 μM quencher-labeled peptide. Data were collected at 25°C with a Jobin Yvon Horiba FluroMax-P fluorescence spectrometer using strain-free quartz cells having a path length of 1 cm. Samples were excited at 315 nm and emission spectra recorded from 350 to 550 nm. Comparisons were made of fluorescence at 412 nm.

Analytical Ultracentrifugation

Peptides or mixtures of peptides at equimolar concentrations, dialyzed against reference buffer (50 mM sodium phosphate, 100 mM NaCl, [pH 7.2]), were spun at 25°C in a Beckman XL-I analytical ultracentrifuge at 40,000, 45,000, and 50,000 rpm for approximately twenty-four hours at each speed. The following concentrations were used: A-Ala, 40, 100, 266 μM; B-Phe, 25 μM; A-Abu, 50, 100, 220 μM; 1:1 A-Ala/B-Phe, 50, 150, 320 μM; 1:1 A-Abu/B-Phe, 50, 150, 320 μM. The contents of each cell were confirmed to be at equilibrium using WINMATCH prior to increasing the speed. Data were analyzed using the programs NONLIN (Johnson et al., 1981) and SEDPHAT (Schuck, 2003; Vistica et al., 2004). Several association models were fit, including a single ideal species, a single nonideal species and different monomer-oligomer equilibria. The results reported in Table 2 are from the model that best fits the data, as indicated. Molecular weights were determined using a partial specific volume, $\bar{\nu}$, calculated by SEDNTERP (Laue et al., 1992).

Crystallization

Crystals were grown using vapor diffusion with hanging-drop geometry from an equimolar mixture of peptides A-Ala and B-Phe (11 mg/ml in 10 mM phosphate at pH 7.2) by mixing 1.5 μl of protein with an equal volume of reservoir solution (100 mM Na HEPES buffer [pH 7.5], 10% *v/v i*-propanol, 20% w/v PEG 4000). Bipyramidal crystals grew after approximately one week.

X-Ray Data Collection and Phasing

Crystals were frozen in a stream of N_2 gas cooled to –180°C using FMS oil (Hampton Research) as a cryoprotectant. A 1.95 Å data set was collected at the Boston University Core Facility for Macromolecular Crystallography using a Rigaku RU-H3RHB X-ray generator with an MSC R-Axis IV++ area detector and 2-theta stage. The DENZO and SCALEPACK packages were used for data indexing, reduction, and scaling (Otwinowski and Minor, 1997). Molecular replacement was performed with MOLREP (Vagin and Teplyakov, 1997). The search model comprised a dimer generated by applying the crystallographic symmetry operators of the BBAT2 structure (PDB ID 1SNE).

Refinement

Manual fitting was performed using SigmaA weighted $2F_o - F_c$ composite-omit and $F_o - F_c$ electron density maps (Read, 1997) in the graphics program O (Jones et al., 1991). Refinement using an MLF target consisted of iterative rounds of minimization and simulated annealing (3000–5000 K) using slow-cool torsional molecular dynamics followed by individual B-factor refinement and manual rebuilding, and was performed until R_{free} ceased to decrease. Water molecules added to the structure were checked by visual inspection of the map at each cycle of refinement. For statistical crossvalidation purposes, 10% of the data was excluded from refinement as a test set (Brünger, 1992, 1997). Topology and parameter files were created for nonstandard groups using bond lengths and angles from the literature (Ali et al., 2004). Values for D-Ala and D-Pro were derived from their L-enantiomers. Analysis of the Ramachandran plot defined by PROCHECK (Laskowski et al., 1993) showed a good final model with 88% of residues in the most favorable regions and 12% of residues in additionally allowed regions. Wilson plot values were calculated using the CCP4 program TRUNCATE (French and Wilson, 1978) with resolution limits 2.5–1.95 Å. The refined structure contained 371 protein atoms and 52 solvent atoms per asymmetric unit (two monomers). Final model statistics are summarized in Table 2. All figures were created using MOLSCRIPT (Kraulis, 1991).

Supplemental Data

Supplemental Data is available online at http://www.structure.org/cgi/content/full/13/2/225/DC1/.

Acknowledgments

We acknowledge the use of the MIT Computational and Systems Biology Initiative High Performance Computing and Proteomics/Structural Biology cores, and we thank Ezra Peisach for helpful discussions, Deborah J. Pheasant for experimental assistance, and Jiangang Chen for contributions to the energy design package. We acknowledge NSF support (CHE 9996335) to B.I. and NIH support to A.E.K. (GM67681) and K.N.A. (GM61099). C.M.T is an Anna Fuller predoctoral fellow.

Received: October 26, 2004
Revised: December 5, 2004
Accepted: December 6, 2004
Published: February 8, 2005

References

Ali, M.H. (2004). The Design and Structural Characterization of Oligomeric Beta Beta Alpha Mini-Proteins. PhD thesis, Massachusetts Institute of Technology, Cambridge, Massachusetts.

Ali, M.H., Peisach, E., Allen, K.N., and Imperiali, B. (2004). X-ray structure analysis of a designed oligomeric miniprotein reveals a discrete quaternary architecture. Proc. Natl. Acad. Sci. USA *101*, 12183–12188.

Beroza, P., and Case, D.A. (1998). Calculations of proton-binding thermodynamics in proteins. Methods Enzymol. *295*, 170–189.

Brooks, B.R., Bruccoleri, R.E., Olafson, B.D., States, D.J., Swaminathan, S., and Karplus, M. (1983). CHARMM. J. Comput. Chem. *4*, 187–217.

Brünger, A.T. (1992). Free R value: a novel statistical quantity for assessing the accuracy of crystal structures. Nature *355*, 472–475.

Brünger, A.T. (1997). Free R value: cross-validation in crystallography. Methods Enzymol. *277*, 366–396.

Cochran, A.G., Skelton, N.J., and Starovasnik, M.A. (2001). Tryptophan zippers: stable, monomeric beta-hairpins. Proc. Natl. Acad. Sci. USA *98*, 5578–5583.

Dahiyat, B.I., and Mayo, S.L. (1997). De novo protein design: fully automated sequence selection. Science *278*, 82–87.

Desjarlais, J.R., and Handel, T.M. (1999). Side-chain and backbone flexibility in protein core design. J. Mol. Biol. *290*, 305–318.

Desmet, J., Maeyer, M.D., Hazes, B., and Lasters, I. (1992). The dead-end elimination theorem and its use in protein side-chain positioning. Nature *256*, 539–542.

Dominy, B.N., and Brooks, C.L. (1999). Development of a generalized Born model parametrization for proteins and nucleic acids. J. Phys. Chem. B *103*, 3765–3773.

Dunbrack, R.L., Jr., and Cohen, F.E. (1997). Bayesian statistical analysis of protein side-chain rotamer preferences. Protein Sci. *6*, 1661–1681.

Dunbrack, R.L., Jr., and Karplus, M. (1993). Backbone-dependent rotamer library for proteins. Application to side-chain prediction. J. Mol. Biol. *230*, 543–574.

Edelhoch, H. (1967). Spectroscopic determination of tryptophan and tyrosine in proteins. Biochemistry *6*, 1948–1954.

Fairman, R., Chao, H.-G., Lavoie, T.B., Villafranca, J.J., Matsueda, G.R., and Novotny, J. (1996). Design of heterotetrameric coiled coils: evidence for increased stabilization by Glu^--Lys^+ ion pair interactions. Biochemistry *35*, 2824–2829.

French, G.S., and Wilson, K.S. (1978). On the treatment of negative intensity observations. Acta Crystallogr. Sect A *34*, 517–525.

Ghirlanda, G., Lear, J.D., Lombardi, A., and DeGrado, W.F. (1998). From synthetic coiled coils to functional proteins: automated design of a receptor for the calmodulin-bonding domain of calcineurin. J. Mol. Biol. *281*, 379–391.

Goldstein, R.F. (1994). Efficient rotamer elimination applied to protein side-chains and related spin glasses. Biophys. J. *66*, 1335–1340.

Harbury, P.B., Zhang, T., Kim, P.S., and Alber, T. (1993). A switch between two-, three-, and four-stranded coiled coils in GCN4 leucine zipper mutants. Science *262*, 1401–1407.

Harbury, P.B., Plecs, J.J., Tidor, B., Alber, T., and Kim, P.S. (1998). High-resolution protein design with backbone freedom. Science *282*, 1462–1467.

Hill, R.B., Raleigh, D.P., Lombardi, A., and DeGrado, W.F. (2000). De novo design of helical bundles as models for understanding protein folding and function. Acc. Chem. Res. *33*, 745–754.

Hodges, R.S. (1996). *De novo* design of α-helical proteins: basic research to medical applications. Biochem. Cell Biol. *74*, 133–154.

Imperiali, B., and Ottesen, J.J. (1999). Uniquely folded mini-protein motifs. J. Pept. Res. *54*, 177–184.

Johnson, M.L., Correia, J.C., Yphantis, D.A., and Halvorson, H.R. (1981). Analysis of data from the analytical ultracentrifuge by nonlinear least-squares techniques. Biophys. J. *36*, 575–588.

Jones, T.A., Zou, J.-Y., Cowan, S.W., and Kjeldgaard, M. (1991). Improved methods for building protein models in electron density maps and the location of errors in these models. Acta Crystallogr. Sect A *47*, 110–119.

Kashiwada, A., Hiroaki, H., Kohda, D., Nango, M., and Tanaka, T. (2000). Design of a heterotrimeric alpha-helical bundle by hydrophobic core engineering. J. Am. Chem. Soc. *122*, 212–215.

Keating, A.E., Malashkevich, V.N., Tidor, B., and Kim, P.S. (2001). Side-chain repacking calculations for predicting structures and stabilities of heterodimeric coiled coils. Proc. Natl. Acad. Sci. USA *98*, 14825–14830.

Kortemme, T., Ramirez-Alvarado, M., and Serrano, L. (1998). Design of a 20-amino acid, three-stranded beta-sheet protein. Science *281*, 253–256.

Kraulis, P.J. (1991). MOLSCRIPT: a program to produce both detailed and schematic plots of protein structures. J. Appl. Crystallogr. *24*, 946–950.

Kuhlman, B., Dantas, G., Ireton, G.C., Varani, G., Stoddard, B.L., and Baker, D. (2003). Design of a novel globular protein fold with atomic-level accuracy. Science *302*, 1364–1368.

Laskowski, R.A., MacArthur, M.W., Moss, D.S., and Thornton, J.M. (1993). Procheck - a program to check the stereochemical quality of protein structures. J. Appl. Crystallogr. *26*, 283–291.

Laue, T.M., Shah, B.D., Ridgeway, T.M., and Pelletier, S.L. (1992). Computer-Aided Interpretation of Analytical Sedimentation Data for Proteins. In Analytical Ultracentrifugation in Biochemistry and Polymer Science, S.E. Harding, A.J. Rowe, and J.C. Horton, eds. (Cambridge, UK: Royal Society of Chemistry), pp. 90–125.

Lazaridis, T., and Karplus, M. (1999). Effective energy function for proteins in solution. Proteins *35*, 133–152.

Lombardi, A., Bryson, J.W., and DeGrado, W.F. (1996). *De novo* design of heterotrimeric coiled coils. Biopolymers *40*, 495–504.

Lombardi, A., Summa, C.M., Geremia, S., Randaccio, L., Pavone, V., and DeGrado, W.F. (2000). Inaugural article: retrostructural analysis of metalloproteins: application to the design of a minimal model for diiron proteins. Proc. Natl. Acad. Sci. USA *97*, 6298–6305.

Marti, D.N., Jelesarov, I., and Bosshard, H.R. (2000). Interhelical ion pairing in coiled coils: solution structure of a heterodimeric leucine zipper and determination of pKa values of Glu side chains. Biochemistry *39*, 12804–12818.

McClain, D.L., Binfet, J.P., and Oakley, M.G. (2001). Evaluation of the energetic contribution of interhelical coulombic interactions for coiled coil helix orientation specificity. J. Mol. Biol. *313*, 371–383.

McDonnell, K.A. (2001). Towards Incorporation of Catalytic Function Into Small Folded Peptide Scaffolds. PhD thesis, Massachusetts Institute of Technology, Cambridge, Massachusetts.

McDonnell, K.A., and Imperiali, B. (2002). Oligomeric beta beta al-

pha miniprotein motifs: pivotal role of single hinge residue in determining the oligomeric state. J. Am. Chem. Soc. *124*, 428–433.

Mezo, A.R., Cheng, R.P., and Imperiali, B. (2001a). Oligomerization of uniquely folded mini-protein motifs: development of a homotrimeric beta beta alpha peptide. J. Am. Chem. Soc. *123*, 3885–3891.

Mezo, A.R., Ottesen, J.J., and Imperiali, B. (2001b). Discovery and characterization of a discretely folded homotrimeric peptide. J. Am. Chem. Soc. *123*, 1002–1003.

Moffet, D.A., Certain, L.K., Smith, A.J., Kessel, A.J., Beckwith, K.A., and Hecht, M.H. (2000). Peroxidase activity in heme proteins derived from a designed combinatorial library. J. Am. Chem. Soc. *122*, 7612–7613.

Moll, J.R., Ruvinov, S.B., Pastan, I., and Vinson, C. (2001). Designed heterodimerizing leucine zippers with a ranger of pIs and stabilities up to 10(-15). M. Protein Sci. *10*, 649–655.

Monera, O., Sonnichsen, F., Hicks, L., Kay, C., and Hodges, R. (1996). The relative positions of alanine residues in the hydrophobic core control the formation of two-stranded or four-stranded alpha-helical coiled-coils. Protein Eng. *9*, 353–363.

Nautiyal, S., and Alber, T. (1999). Crystal structure of a designed, thermostable, heterotrimeric coiled coil. Protein Sci. *8*, 84–90.

Nautiyal, S., Woolfson, D.N., King, D.S., and Alber, T. (1995). A designed heterotrimeric coiled coil. Biochemistry *34*, 11645–11651.

Neidigh, J.W., Fesinmeyer, R.M., and Andersen, N.H. (2002). Designing a 20-residue protein. Nat. Struct. Biol. *9*, 425–430.

O'Shea, E.K., Lumb, K.J., and Kim, P.S. (1993). Peptide 'Velcro': design of a heterodimeric coiled coil. Curr. Biol. *3*, 658–667.

O'Shea, E.K., Rutkowski, R., and Kim, P.S. (1992). Mechanism of specificity in the Fos-Jun oncoprotein heterodimer. Cell *68*, 699–708.

Ottesen, J.J., and Imperiali, B. (2001). Design of a discretely folded mini-protein motif with predominantly beta-structure. Nat. Struct. Biol. *8*, 535–539.

Otwinowski, Z., and Minor, W. (1997). Processing of x-ray diffraction data collected in oscillation mode. Methods Enzymol. *276*, 307–326.

Petka, W.A., Harden, J.L., McGrath, K.P., Wirtz, D., and Tirrell, D.A. (1998). Reversible hydrogels from self-assembling artificial proteins. Science *281*, 389–392.

Read, R.J. (1997). Model phases: probabilities and bias. Methods Enzymol. *278*, 110–128.

Rivas, G., and Minton, A.P. (2003). Tracer sedimentation equilibrium: a powerful tool for the quantitative characterization of macromolecular self- and hetero-associations in solution. Biochem. Soc. Trans. *31*, 1015–1019.

Ryadnov, M.G., and Woolfson, D.N. (2003). Engineering the morphology of a self-assembling protein fibre. Nat. Mater. *2*, 329–332.

Schnarr, N.A., and Kennan, A.J. (2003). Specific control of peptide assembly with combined hydrophilic and hydrophobic interfaces. J. Am. Chem. Soc. *125*, 667–671.

Schuck, P. (2003). On the analysis of protein self-association by sedimentation velocity analytical ultracentrifugation. Anal. Biochem. *320*, 104–124.

Sia, S.K., and Kim, P.S. (2001). A designed protein with packing between left-handed and right-handed helices. Biochemistry *40*, 8981–8989.

Snow, C.D., Nguyen, H., Pande, V.S., and Gruebele, M. (2002). Absolute comparison of simulated and experimental protein-folding dynamics. Nature *420*, 102–106.

Struthers, M.D., Cheng, R.P., and Imperiali, B. (1996). Design of a monomeric 23-residue polypeptide with defined tertiary structure. Science *271*, 342–345.

Struthers, M.D., Ottesen, J.J., and Imperiali, B. (1998). Design and NMR analyses of compact, independently folded BBA motifs. Fold. Des. *3*, 95–103.

Vagin, A., and Teplyakov, A. (1997). MOLREP: an automated program for molecular replacement. J. Appl. Crystallogr. *30*, 1022–1025.

Vistica, J., Dam, J., Balbo, A., Yikilmaz, E., Mariuzza, R.A., Roualt, T.A., and Schuck, P. (2004). Sedimentation equilibrium analysis of protein interactions with global implicit mass conservation constraints and systematic noise decomposition. Anal. Biochem. *326*, 234–256.

Walshaw, J., and Woolfson, D.N. (2001). Socket: a program for identifying and analysing coiled-coil motifs within protein structures. J. Mol. Biol. *307*, 1427–1450.

Zagrovic, B., and Pande, V.S. (2003). Structural correspondence between the alpha-helix and the random-flight chain resolves how unfolded proteins can have native-like properties. Nat. Struct. Biol. *10*, 955–961.

Zhou, N.E., McKay, C., and Hodges, R.S. (1992). Synthetic model proteins: the relative contributions of leucine residues at the nonequivalent positions of the 3–4 hydrophobic repeat to the stability of the two-stranded α-helical coiled coil. Biochemistry *31*, 5739–5746.

Zhou, N.E., Kay, C.M., and Hodges, R.S. (1994). The role of interhelical ionic interactions in controlling protein folding and stability. *De novo* designed synthetic two-stranded α-helical coiled coils. J. Mol. Biol. *237*, 500–512.

Zondlo, N.J., and Schepartz, A. (1999). Highly specific DNA recognition by a designed miniature protein. J. Am. Chem. Soc. *121*, 6938–6939.

Accession Numbers

Coordinates of the refined structure of BBAhetT1 have been deposited with the Protein Data Bank (accession code 1XOF).